Geometric shapes describing nuclear reaction mechanisms such as fusion, alpha emission and capture, binary and ternary fission, planar fragmentation and n-alpha nuclei

G. Royer, J. Jahan and N. Mokus
Subatech laboratory, UMR : IN2P3/CNRS-University-IMT, Nantes, France

Abstract
Different shape sequences useful to describe simply the fusion, alpha emission or capture, binary and ternary fission, planar and three dimensional fragmentation and n-alpha nuclei are gathered together. Their geometric characteristics allowing to determine the total energy and the dynamics of a nuclear system are provided, mainly the volume, the surface, the Coulomb function, the moments of inertia, the quadrupole moment and the rms radius.

1 Introduction

To describe macroscopically nuclear reaction mechanisms such as fusion [1], alpha emission and capture [2], binary and ternary fission [3], fragmentation [4] and n-alpha nuclei [5,6] one simulates the nuclear system by geometric shapes [7,8] and determines the main geometric characteristics such as volume, surface, Coulomb function, moments of inertia, quadrupole moment and rms radius. In this work, the following shapes will be investigated: elliptic and hyperbolic lemniscatoids, prolate compact ternary shapes, tori and bubbles.

Other multibody shapes such as linear chain, triangle, square, tetrahedron, pentagon, trigonal bipyramid, square pyramid, hexagon, octahedron, octagon and cube used to describe some light nuclei as alpha molecules have been used recently [5,6].

2 Elliptic lemniscatoids and pumpkin-like shapes

The fusion, alpha and cluster radioactivities and fission through compact shapes lead, in first approximation, from one sphere to two tangent spheres or vice-versa. Such a deformation valley can be simulated using two halves of different elliptic lemniscatoids. An elliptic lemniscatoid is the inverse of an oblate ellipsoid. One elliptic lemniscate is defined, in polar coordinates, by

$$R(\theta)^2 = a^2 \sin^2 \theta + c^2 \cos^2 \theta, \tag{1}$$

and the equation of the elliptic lemniscatoid is

$$a^2 x^2 + a^2 y^2 + c^2 z^2 = (x^2 + y^2 + z^2)^2, \tag{2}$$

where the z axis is the axis of revolution. Assuming volume conservation, the ratio $s = a/c$ of the neck radius to the half-elongation of the system defines completely the shape. When s decreases from 1 to 0 the lemniscatoid varies continuously from a sphere to two tangent equal spheres. When the perpendicular x axis is taken as axis of revolution the elliptic lemniscates generate pumpkin-like configurations (see Fig. 1). For the elliptic lemniscatoid the volume and surface are given by

$$Vol = \frac{4}{3}\pi R_0{}^3 = \frac{\pi}{12}c^3 \left[4 + 6s^2 + \frac{3s^4}{\sqrt{1-s^2}} \sinh^{-1}\left(\frac{2}{s^2}\sqrt{1-s^2} \right) \right], \tag{3}$$

$$S = 4\pi R_0{}^2 B_s = 2\pi c^2 \left[1 + \frac{s^4}{\sqrt{1-s^4}} \sinh^{-1}\left(\frac{1}{s^2}\sqrt{1-s^4} \right) \right], \tag{4}$$

Fig. 1: Evolution of the elliptic lemniscatoids generates by a revolution of the lemniscates around the horizontal axis and of the pumpkin-like shapes generates by a revolution around the vertical axis.

R_0 being the radius of the initial or final sphere and B_s the dimensionless surface function.
r, the distance between the mass centres of the right and left parts of the object, is given by

$$r = \pi c^4 \frac{1 + s^2 + s^4}{3V}. \tag{5}$$

The dimensionless perpendicular and parallel moments of inertia (relatively to the moment of inertia of the equivalent sphere $\frac{2}{5}mR_0^2$) are expressed as

$$I_{\perp,rel} = \frac{c^5 s^2}{512(1-s^2)R_0^5}\left[\frac{112}{s^2} + 8 + 30s^2 - 135s^4 + \frac{120s^4 - 135s^6}{\sqrt{1-s^2}}\sinh^{-1}\left(\sqrt{\frac{1-s^2}{s^2}}\right)\right]. \tag{6}$$

$$I_{\parallel,rel} = \frac{c^5 s^2}{512(1-s^2)R_0^5}\left[\frac{32}{s^2} + 48 + 100s^2 - 210s^4 + \frac{240s^4 - 210s^6}{\sqrt{1-s^2}}\sinh^{-1}\left(\sqrt{\frac{1-s^2}{s^2}}\right)\right]. \tag{7}$$

The dimensionless quadrupole moment is

$$Q = \frac{\pi c^5 s^2}{96(1-s^2)R_0^5}\left[\frac{16}{s^2} - 8 - 14s^2 + 15s^4 - \frac{24s^4 - 15s^6}{\sqrt{1-s^2}}\sinh^{-1}\left(\sqrt{\frac{1-s^2}{s^2}}\right)\right]. \tag{8}$$

Similar formulas are available for the pumpkin-like shapes [7].

To generalize the elliptic lemniscatoid shape sequence to asymmetric but axially symmetric shapes it is sufficient to join two halves of different elliptic lemniscatoids assuming the same transverse distance a (see Fig. 2 and [1, 7]) and two different c_1 and c_2 half elongations and two different ratios $s_1 = a/c_1$ and $s_2 = a/c_2$.
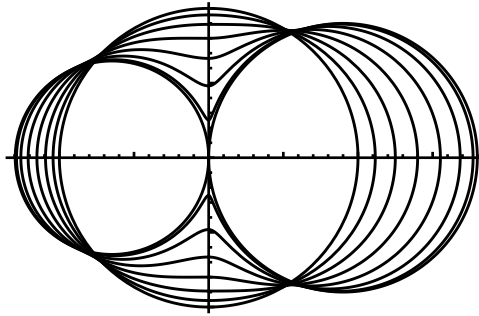

Fig. 2: Two parameter shape sequence varying from two touching unequal spheres to one sphere or vice versa.

3 Hyperbolic lemniscatoids

The most commonly admitted fission path corresponds to elongated shapes with shallow necks. It can be simulated, in first approximation, by hyperbolic lemniscatoids.

For the one-body configurations the hyperbolic lemniscatoids are defined by

$$x^2 = -z^2 + 0.5c^2(s^2 - 1) + 0.5c\sqrt{8(1 - s^2)z^2 + c^2(1 + s^2)^2}. \tag{9}$$

For the two-body shapes the separated ovals are given by

$$x^2 = -z^2 - 0.5c^2(s^2 + 1) + 0.5c\sqrt{8(1 + s^2)z^2 + c^2(1 - s^2)^2}. \tag{10}$$

Assuming the volume conservation, these shapes are one-parameter dependent. The ratio of the minor and major axes $s = a/c$ can be used for the one-body shapes. When the ovals are separated, the opposite s of the ratio of the distance between the tips of the fragments and the system elongation can be retained (see Fig. 3). When s varies from 1 to -1 the shapes evolves from one sphere to two infinitely separated spheres. The volume of the system is, respectively for the one-body and two-body shapes:
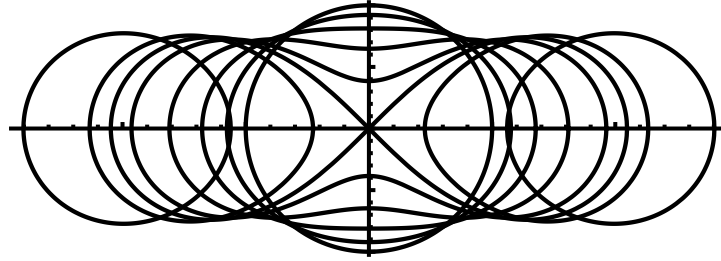

Fig. 3: Hyperbolic lemniscatoid shape sequence. At the scission point, the configuration is the Bernoulli lemniscate.

$$Vol = \frac{\pi c^3}{12} \left[-2 + 6s^2 + 3\frac{(1 + s^2)^2}{\sqrt{2(1 - s^2)}} \sinh^{-1}\left(\frac{2\sqrt{2(1 - s^2)}}{1 + s^2}\right) \right], \tag{11}$$

$$Vol = \frac{\pi c^3}{12} \left[-2(1 + s)^3 + 3\frac{(1 - s^2)^2}{\sqrt{2(1 + s^2)}} \sinh^{-1}\left(\frac{2(1 + s)\sqrt{2(1 + s^2)}}{(1 - s)^2}\right) \right]. \tag{12}$$

For the one-body shapes, the relative surface function reads

$$B_s = \frac{c^2}{4R_0{}^2} \times \left[4(1 + s^2) + 2\sqrt{\frac{2(1 + s^2)}{1 - s^2}} s^2 F\left(\sin^{-1}\sqrt{1 - s^2}, \frac{1}{\sqrt{1 + s^2}}\right) \right.$$
$$\left. - 2(1 + s^2)\sqrt{\frac{2(1 + s^2)}{1 - s^2}} E\left(\sin^{-1}\sqrt{1 - s^2}, \frac{1}{\sqrt{1 + s^2}}\right) \right]. \tag{13}$$

E and F are incomplete elliptic integrals [7]. B_s is calculated numerically for the two-body configuration. The distance r between the centres of the right and left parts is for the one and two-body shapes

$$r = \frac{c^4}{8R_0{}^3} \times (1 + 4s^2 + s^4) \tag{14}$$

$$r = \frac{c^4}{8R_0{}^3} \times \frac{(1 - s^2)^3}{1 + s^2}. \tag{15}$$

For the one-body shapes the parallel and perpendicular moments of inertia and the quadrupole moment are given by

$$I_\parallel = \frac{c^5}{512(1-s^2)R_0{}^5} \times \left[147 - 27s^2 - 15s^4 - 225s^6 \right. \tag{16}$$
$$\left. - \frac{15(1+s^2)^2(15-34s^2+15s^4)}{2\sqrt{2(1-s^2)}} \sinh^{-1}\left(\frac{2\sqrt{2(1-s^2)}}{1+s^2}\right)\right],$$

$$I_\perp = \frac{c^5}{1024(1-s^2)R_0{}^5} \times \left[269 + 251s^2 - 145s^4 - 255s^6 \right. \tag{17}$$
$$\left. - \frac{15(1+s^2)^2(17-30s^2+17s^4)}{2\sqrt{2(1-s^2)}} \sinh^{-1}\left(\frac{2\sqrt{2(1-s^2)}}{1+s^2}\right)\right],$$

$$Q = \frac{\pi c^5}{192(1-s^2)R_0{}^5} \times \left[-5 + 61s^2 - 23s^4 + 39s^6 \right. \tag{18}$$
$$\left. + \frac{3(1+s^2)^2(13-38s^2+13s^4)}{2\sqrt{2(1-s^2)}} \sinh^{-1}\left(\frac{2\sqrt{2(1-s^2)}}{1+s^2}\right)\right].$$

For the two-body shapes these quantities are expressed as

$$I_\parallel = \frac{c^5}{512(1+s^2)R_0{}^5} \times \left[147 + 225s + 27s^2 - 15s^3 - 15s^4 + 27s^5 + 225s^6 + 147s^7 \right. \tag{19}$$
$$\left. - \frac{15(1-s^2)^2(15+34s^2+15s^4)}{2\sqrt{2(1+s^2)}} \sinh^{-1}\left(\frac{2(1+s)\sqrt{2(1+s^2)}}{(1-s)^2}\right)\right],$$

$$I_\perp = \frac{c^5}{1024(1+s^2)R_0{}^5} \times \left[269 + 255s - 251s^2 - 145s^3 - 145s^4 - 251s^5 + 255s^6 \right. \tag{20}$$
$$\left. + 269s^7 - \frac{15(1-s^2)^2(17+30s^2+17s^4)}{2\sqrt{2(1+s^2)}} \sinh^{-1}\left(\frac{2(1+s)\sqrt{2(1+s^2)}}{(1-s)^2}\right)\right],$$

$$Q = \frac{\pi c^5}{192(1-s^2)R_0{}^5} \times \left[-5 - 39s - 61s^2 - 23s^3 - 23s^4 - 61s^5 - 39s^6 - 5s^7 \right. \tag{21}$$
$$\left. + \frac{3(1-s^2)^2(13+38s^2+13s^4)}{2\sqrt{2(1+s^2)}} \sinh^{-1}\left(\frac{2(1+s)\sqrt{2(1+s^2)}}{(1-s)^2}\right)\right].$$

4 Comparison between the elliptic lemniscatoid and hyperbolic lemniscatoid shape valleys

In nuclear physics the question of reversibility of the fission and fusion mechanisms was a focus of discussions already in 1939 between Fermi and Bohr. The different possible shapes taken by a fissioning nucleus were firstly explore using a development of the radius in terms of Legendre polynomials, thinking that the fission process is only governed by the balance between the repulsive Coulomb forces and the attractive surface tension forces. This method leads naturally to smooth elongated one-body configurations resembling to hyperbolic lemniscatoids. This development cannot simulate strongly distorted shapes and the rupture into compact fragments or the alpha decay or capture and cluster radioactivity.

Furthermore, within liquid drop models, to reproduce the fusion data and the alpha and cluster radioactivities one must introduce an additional term, the so-called proximity energy, to take into account the strong nuclear interaction between nucleons of the surfaces in regard between almost spherical nuclei or in a deep crevice in one-body shapes. This proximity energy is evidently very small for elongated shapes with shallow necks and, then, it is often neglected but this term is important in fusion or fission through compact and creviced shapes. It exists a degeneracy in energy between these two deformation valleys. The main available experimental data are the moments of inertia and quadrupole moments and it has been shown that they are similar in the two paths [9].

5 Prolate ternary shapes

One of the hypotheses to explain the nucleosynthesis in stars is the ternary fusion of three alpha particles to form the ^{12}C nucleus. In the decay channels the ternary fission has been observed even though its probability is much lower than the one of the binary fission. From the asymmetric binary shapes one may generate prolate ternary shapes (see Fig. 4) in cutting the smallest fragment along its maximal transverse distance by a symmetry plane. The shape is still only two-parameter dependent. For $s_1=s_2=1$ the shape corresponds to the initial or final sphere and for $s_1=s_2=0$ two spheres of radius R_1 are aligned with a central smaller sphere of radius R_2.
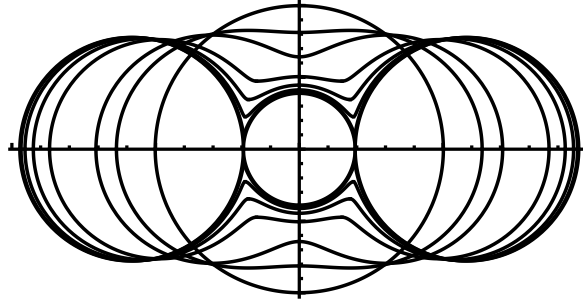

Fig. 4: Evolution of the shape from a sphere to two equal spheres aligned with a smaller sphere between them.

6 Tori and bubbles

Beyond the pumpkin like shapes, ring torus may appear to finally desintegrate into n fragments emitted roughly in the same plane (see Fig. 5). The dimensionless parameter s_t allows to follow this evolution

$$s_t = (r_t - r_s)/2r_s, \tag{22}$$

where r_s and r_t are the sausage and torus radii.
The different geometric characteristics are given by

$$Vol = \frac{4\pi R_0^3}{3} = 2\pi^2 r_t r_s^2 = \frac{\pi^2 c_t^3}{4}(1 + 2s_t), \tag{23}$$

$$I_{\perp,rel} = \frac{35}{32}(1 + 3s_t + 3s_t^2)\left(\frac{16}{3\pi(1 + 2s_t)}\right)^{2/3}, \tag{24}$$

$$\langle r^2 \rangle_{rel} = \frac{5}{6}(1 + 2s_t + 2s_t^2)\left(\frac{16}{3\pi(1 + 2s_t)}\right)^{2/3}, \tag{25}$$

$$B_s = \frac{4\pi^2 r_s r_t}{4\pi R_0{}^2} = \frac{\pi c_t{}^2}{4R_0{}^2}(1 + 2s_t), \tag{26}$$

$$r_s = R_0 \left(\frac{2}{3\pi(1 + 2s)} \right)^{1/3}. \tag{27}$$

Bubbles of thick skin are often formed within violent reactions where the out of equilibrium effects play an essential role. Calculations within bubbles of constant density can give a first rough approach of the more complex reality [7]. Assuming volume conservation, the bubble characteristics can be calculated from the ratio $p = r_1/r_2$ of the inner and outer radii.
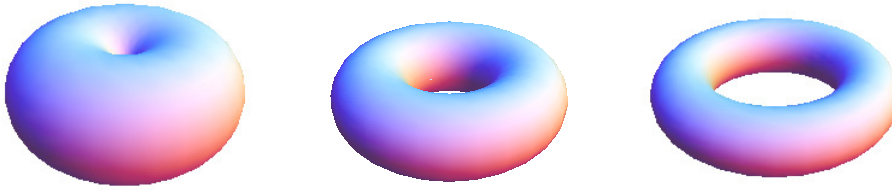

Fig. 5: Evolution of the torus configuration.

7 n-alpha nuclei

Within an α-particle model the energy of the ^{12}C, ^{16}O, ^{20}Ne, ^{24}Mg and ^{32}S nuclei has been determined assuming different α-molecule configurations: linear chain, triangle, square, tetrahedron, pentagon, trigonal bipyramid, square pyramid, hexagon, octahedron, octagon, and cube [6].

8 Conclusion

Different shape sequences are proposed to describe simply the alpha emission or absorption, cluster radioactivity, fusion, fission, fragmentation and n-alpha nuclei. Their geometric definitions and properties are provided, mainly, the volume, the surface, the Coulomb function, the moments of inertia, the quadrupole moment and the rms radius. Within a liquid drop model approach, the total energy of a nuclear system, the dynamics of the processes and the angular distribution of the fragments may be determined.

References

[1] G. Royer and B. Remaud, *Nucl. Phys. A* **444** (1985) 477.

[2] G. Royer, *J. Phys. G: Nucl. Part. Phys.* **26** (2000) 1149.

[3] G. Royer, M. Jaffré, and D. Moreau, *Phys. Rev. C* **86** (2012) 044326.

[4] C. Fauchard and G. Royer, *Nucl. Phys. A* **598** (1996) 125.

[5] G. Royer, A. Escudie, and B. Sublard, *Phys. Rev. C* **90** (2014) 024607.

[6] G. Royer, G. Ramasamy, and P. Eudes, *Phys. Rev. C* **92** (2015) 054308.

[7] G. Royer, N. Mokus, and J. Jahan, *Phys. Rev. C* **95** (2017) 054610.

[8] R. W. Hasse and W. D. Myers, Geometrical Relationships of Macroscopic Nuclear Physics, 1988 (Springer verlag, Berlin).

[9] J. Mignen, G. Royer, and F. Sebille, *Nucl. Phys. A* **489** (1988) 461.